Available online at www.sciencedirect.com
ScienceDirect
Journal of Power Sources 161 (2006) 432–436
JOURNAL OF POWER SOURCES
www.elsevier.com/locate/jpowsour

Development of a miniaturized polymer electrolyte membrane fuel cell with silicon separators

Jun-Yeop Kim, Oh Joong Kwon, Sun-Mi Hwang, Moo Seong Kang, Jae Jeong Kim *

Research Center for Energy Conversion and Storage, School of Chemical and Biological Engineering, Seoul National University, Shillim-dong, Kwanak-gu, Seoul 151-742, Republic of Korea

Received 7 March 2006; received in revised form 19 April 2006; accepted 19 April 2006
Available online 12 June 2006

Abstract

The fabrication process and electrochemical characterization of a miniaturized PEM fuel cell with silicon separators were investigated. Silicon separators were fabricated with silicon fabrication technologies such as by photolithography, anisotropic wet etching, anodic bonding and physical vapor deposition (PVD). A 400 μm × 230 μm flow channel was made with KOH wet etching on the front side of a silicon separator, and then a 550 nm gold current collector and 350 nm TiN_x thin film heater were respectively formed on the front side and the opposite side by PVD. Two separators were assembled with the membrane electrode assembly (MEA) having a 4 cm^2 active area for the single cell. With pure hydrogen and oxygen under atmospheric pressure without humidification, the performance of the single fuel cell was measured. A single cell operation led to generation of 203 mW cm^{-2} at 0.6 V at room temperature, which corresponded to 360 mW cm^{-3} in terms of volumetric fuel cell power density, with 20 ccm of gas flow rate of hydrogen and oxygen at the inlet.

Keywords: Miniaturized fuel cell; PEMFC; Separator; Silicon technology; PtRu catalyst

1. Introduction

Proton exchange membrane (PEM) fuel cells have been developed by many research groups as a potential candidate for stationary and portable applications because of their many advantages: high efficiency, high energy density, low operating temperature, low noise, rapid recharging and no emission of polluting materials using hydrogen [1,2]. With intensive study, there has been much improvement, but many problems remain unsolved. One such problem is the heavy weight and large volume of the graphite plate, because it makes the fuel cell bulky for portable application.

Conventional PEM fuel cells are composed of machined or pressure-molded bipolar plates made of graphite or a carbon-polymer composite or a metal [3]. Those kinds of bipolar plates normally have large dimensions and are heavy. Therefore, they are not applicable when it comes to downsizing PEM fuel cells. Thus other materials have been tried for the separator or bipolar plate materials in miniaturized fuel cells.

Silicon is one of the candidate materials for the separator in miniaturized fuel cells. It has a low density as well as satisfying the requirements for the separator. Silicon has a low gas permeability, high thermal conductivity, and processability with semiconductor processing technologies [4,5]. Additionally, if a gold film is deposited on the silicon separator, the silicon separator can have a high electrical conductivity and high chemical stability in the presence of both fuel and oxidant.

Until now, many groups have tried unsuccessfully to get a comparable power density to the conventional fuel cell using silicon [5–8]. The aim of this study was also to gain comparative result to the conventional non-silicon fuel cell. However, this study was more focused on the substitution of a graphite plate by a silicon plate reinforced with Pyrex and with a Au current collector, and to test the possibility of a thin film heater. The performance tests were carried out by varying the compaction pressure, gas flow rate and cell temperature. An optimum condition for the single fuel cell found.

* Corresponding author. Tel.: +82 2 880 8863; fax: +82 2 888 2705.
E-mail address: jjkimm@snu.ac.kr (J.J. Kim).

0378-7753/$ – see front matter © 2006 Elsevier B.V. All rights reserved.
doi:10.1016/j.jpowsour.2006.04.102

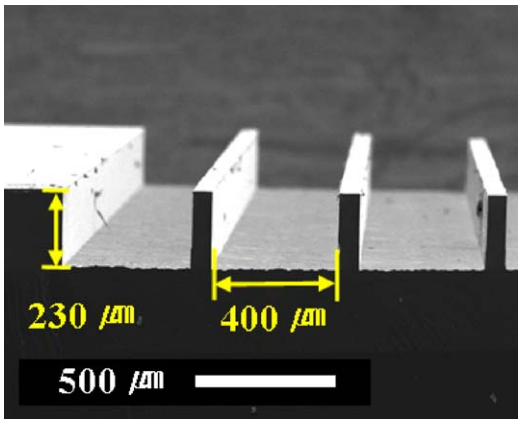

Fig. 1. Silicon wafer with micro-channels formed by a KOH wet etching process.

2. Experimental

2.1. Fabrication of a silicone separator

Micro-channels on a silicon separator were created by a photolithographic process [9]. A (1 1 0) orientation silicon wafer with a 525 ± 25 μm thickness was used to form micro-channels, which had a rectangular cross sectional profile. On the front side of the thermally-oxidized silicon wafer, a photoresist was spin-coated for the etching mask. After UV exposure and SiO_2 removal, Si wet etching was performed with a 30 wt.% KOH solution at 80 °C as shown in Fig. 1. As a result, micro-channels with 400 μm width and 230 μm depth were made on the separators.

After finishing the formation of the micro-channel, anodic bonding was carried out to attach a 500 μm Pyrex wafer on the back side of the silicon wafer to increase the physical strength of the silicon separator. The flexural (three-point bending) test with a specimen of 20 mm span and 3 mm width was performed with a LLOYD LF-Plus universal testing machine at room temperature to confirm strength improvement.

A gold film was formed on the Ta layer, which was introduced to increase the adhesion strength between the gold and silicon.

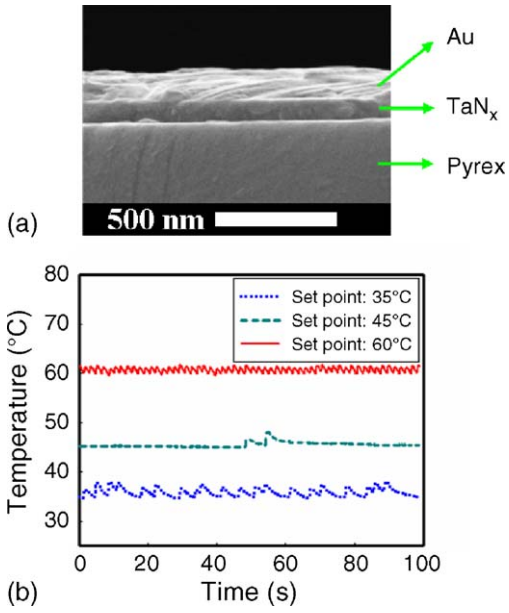

Fig. 3. Thin film heater for cell temperature control. (a) 380 nm Au/Ta/TaN_x layers as a thin film heater deposited on Pyrex substrate and (b) The result of temperature control with a thin film heater at 35 °C, 45 °C, and 60 °C.

Both of them were deposited by DC magnetron sputtering as shown in Fig. 2. Gold had a 550 nm thickness and Ta had a 20 nm thickness.

A thin-film heater was fabricated on the Pyrex surface to control the temperature of the single fuel cell. Firstly, a 80 nm thick TaN_x layer was deposited for the heater, and then a 300 nm gold layer was sputtered onto the restricted region as a contact pad. Subsequently, an annealing step followed to enhance the adhesion of the metal layers. Fig. 3(a) shows the SEM image of a cross section of the thin film heater, and Fig. 3(b) shows its ability to control the temperature with a maximum deviation of about 4 °C.

2.2. MEA preparation

The MEA was prepared in a conventional way. Carbon papers without a wet-proof treatment (Toray TGPH-090, 260 μm) were

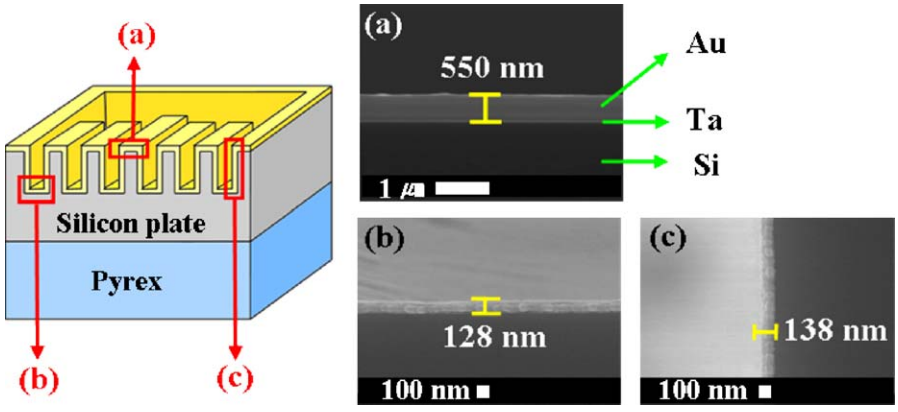

Fig. 2. Second electron microscopy (SEM) images of the Au/Ta layers deposited on a patterned silicon plate. Au layer on the top side of a silicon plate was about 550 nm and formed a continuous film on each surface.

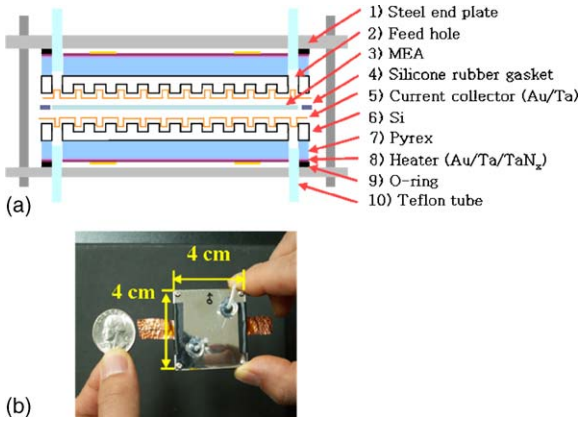

Fig. 4. Single fuel cell with silicon separators. (a) Cross section schematic diagram and (b) real features of the assembled single fuel cell.

used for the GDL, and PtRu/C (HISPEC 5000, from Johnson Matthey) was applied as the anode catalyst because our fuel cell will be combined with a silicon-based miniature reformer in the near future [10]. On the cathode GDL, Pt/C (C1-40, E-TEK) was chosen. A spray coating method with an air-brush was employed to form the catalyst layer on the GDLs. The anode and cathode catalyst weight were 0.375 mg cm^{-2} of PtRu/C (Pt 0.25 mg cm^{-2}) and 0.4 mg cm^{-2} Pt/C, respectively. On both catalyst layers, 0.3 mg cm^{-2} of Nafion was impregnated.

A Nafion 112 (EW 1100, Dupont) membrane was pretreated with H_2O_2, H_2SO_4 solution and deionized (D.I.) water, then hot-pressed at 120 °C and 2 MPa. Finally, 4 cm^2 MEA was prepared for the fuel cell performance test.

2.3. Single fuel cell assembly

A schematic diagram of the silicon-based miniaturized PEM fuel cell structure with a 2.8 mm metal end plate is shown in Fig. 4(a). Copper foils were connected for the conduction of electrons generated at the MEA, and a 0.5 mm silicon rubber gasket was used to seal between two silicon polar plates. Fig. 4(b) shows the real features of an assembled miniature fuel cell.

2.4. The measurement of cell performance

The fuel cell was activated by cycling the potential with pure hydrogen and oxygen. Then the same gases were used as a fuel and an oxidant under atmospheric pressure for measurement of the cell performance at room temperature. In the temperature effect experiment, a temperature controller was introduced to precisely control the temperature of the single cell. The temperature controller consisted of a relay and a power supply. The flow rates of hydrogen and oxygen were controlled with a mass flow meter/controller (EL-Flow®, Bronkhorst High-Tech). An electrical load system (EL-200P, Deagil electronics Co., LTD) in a constant current mode was used to measure both the polarization curves and the power density curves in this study.

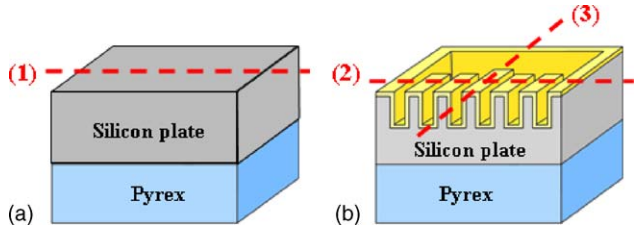

Fig. 5. Schematic diagram of the flexural test direction on (a) bare plate and (b) patterned plate.

3. Results and discussion

3.1. The flexural strength of a silicon separator

For use as a separator by substituting graphite plate and other composite material plates, a silicon separator should have a comparable strength to the graphite plate [11]. For that purpose, the silicon plate was reinforced by bonding Pyrex onto the back side of the silicon plate. Pyrex compensated for the brittleness of the silicon plate, thus giving more strength to silicon plate.

The mechanical properties of the silicon separator combined with Pyrex were measured using a flexural test with a universal testing machine. Three specimens of bare and patterned plate were prepared for this test. Fig. 5 shows the schematic diagrams of the flexural test direction. The strength of each specimen was measured to be 244.8, 111.5 and 56.5 MPa, respectively. The weakest direction was parallel to the patterned channel. Even the weakest direction, however, had a strength sufficient to satisfy the required strength of a conventional composite bipolar plate.

3.2. Evaluation of cell performance

3.2.1. Compression pressure of the miniaturized fuel cell

The performance of fuel cells is normally affected by compression pressure. The performance of a fuel cell is proportional to the compression pressure within some pressure range [12]. And this is also true in silicon-based miniaturized fuel cell.

To test the compression pressure effect on the performance of our silicon-based miniaturized fuel cell, a torque driver was used to measure the compression pressure. Fig. 6 shows the results

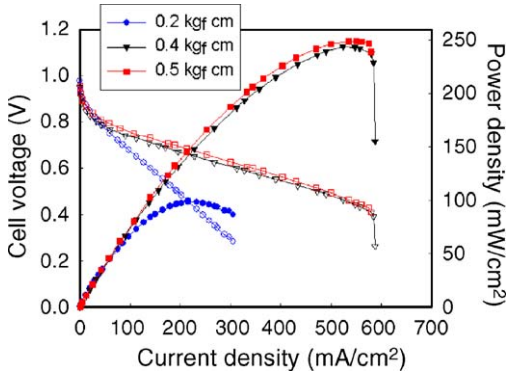

Fig. 6. The performance of a single fuel cell with various compaction pressures at room temperature and atmospheric pressure. Both H_2 and O_2 gas flow rates were 20 ccm. (Cell voltage: open, power density: solid).

obtained by varying the compression pressure. The performance was proportional up to 0.5 kg_f cm (63.9 N cm^{-2}), but not over 0.5 kg_f cm. 0.5 mm silicon rubber gasket was introduced not only as a sealing material but also as a thickness gap limiter to prevent the channel wall from collapsing in this study. Thus the performance of the fuel cell was stabilized around 0.5 kg_f cm due to the thickness controling effect of the silicon rubber gasket.

3.2.2. *Effect of gas flow rates*

Fig. 7(a) shows the cell performance with different hydrogen flow rates at room temperature when the oxygen flow rate was fixed at 20 ccm. As the hydrogen flow rate was increased from 10 to 40 ccm, the I–V curve clearly demonstrated a shift of the mass transport limitation to higher current density, which increased from 300 to 800 mA cm^{-2}. But there was no change in power density at 0.6 V. On the other hand, Fig. 7(b) shows that the maximum current density hardly changed even though the oxygen flow rate was increased from 10 to 40 ccm. This means that the reaction occurring at cathode is not controlled by the mass transfer limitation of oxygen, but by the proton flow from anode through the Nafion membrane. The maximum current density increase of the single fuel cell in Fig. 7(a) could be explained in terms of gas utilization and its consumption. In Table 1(a) utilization of the H_2 gas was gradually decreased from 87.6% to 58.5% with increase of gas flow rate, but its consumption increased from 8.76 to 23.4 ccm. At the same time, the O_2 gas consumption rate increased from 4.51 to 12.0 ccm according to the hydrogen consumption even at a fixed oxygen flow rate of 20 ccm as shown in Table 1(a). This means that the performance of the miniaturized fuel cell was mainly controlled by the mass transfer of hydrogen. This is more clear from Table 1(b) and Fig. 7(b). In contrast to the result of Table 1(a) and Fig. 7(a), consumption of oxygen and the maximum current density did not change in Table 1(b) and Fig. 7(b), despite the increase of oxygen flow from 10 to 40 ccm. This result is also evidence of that the performance of a miniaturized fuel cell is controlled by the hydrogen supply in this study.

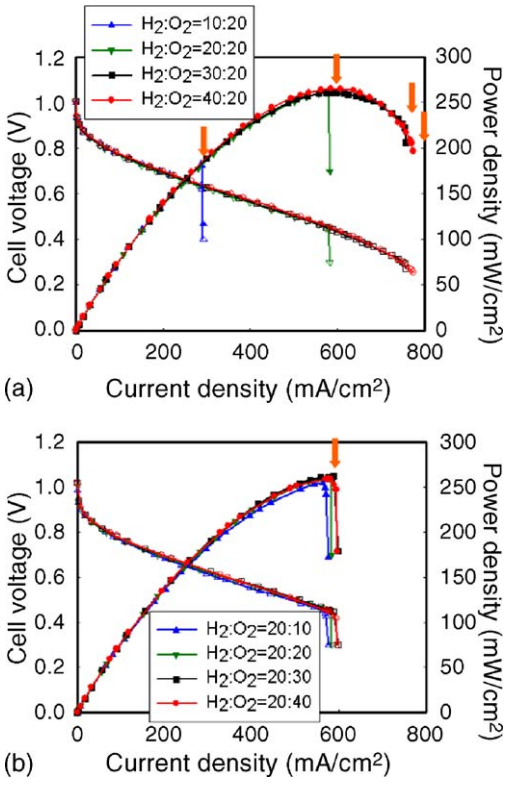

Fig. 7. The performance of single fuel cell when each gas feed rate was increased from 10 to 40 ccm at room temperature and atmospheric pressure. (Cell voltage: open, power density: solid).

Based on the above results, the hydrogen and oxygen flow rate for the performance test was selected to be 20 ccm by considering the utilization of reactant and the operation range of the fuel cell. A single fuel cell demonstrated a 261.0 mW cm^{-2} maximum power density at 0.454 V and 202.8 mW cm^{-2} power density at 0.6 V with 20 ccm hydrogen and oxygen flow rates.

Table 1
Utilization and gas consumption at maximum current density according to the change of gas flow rates

Flow rates (ccm)	H_2 gas feed		O_2 gas (20 ccm)	
	Utilization (%)	Consumption (ccm)	Utilization (%)	Consumption (ccm)
(a) Varying H_2 flow rate with 20 ccm O_2 gas				
10	87.6	8.76	22.6	4.51
20	87.6	17.52	45.1	9.01
30	76.0	22.80	58.5	11.7
40	58.5	23.40	60.0	12.0
Flow rates (ccm)	O_2 gas feed		H_2 gas (20 ccm)	
	Utilization (%)	Consumption (ccm)	Utilization (%)	Consumption (ccm)
(b) Varying O_2 flow rate with 20 ccm H_2 gas				
10	88.6	8.86	86.1	17.22
20	45.1	9.02	87.6	17.51
30	30.4	9.13	88.7	17.74
40	23.0	9.21	89.5	17.90

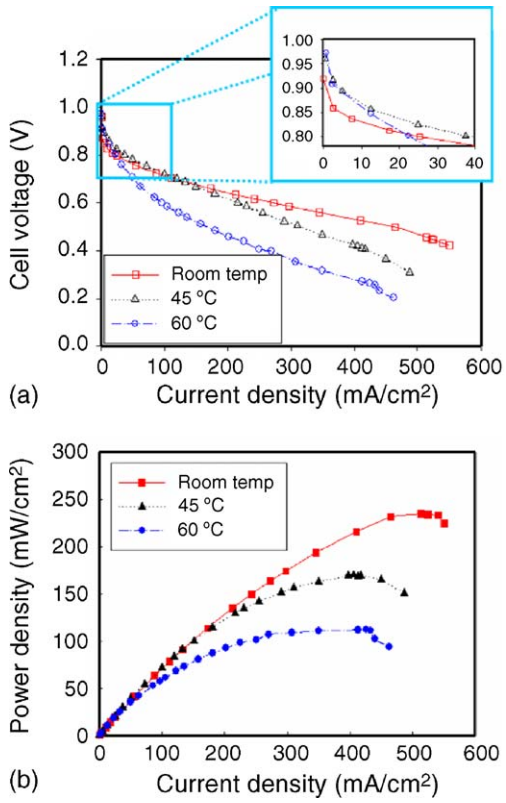

Fig. 8. The performance of a single fuel cell according cell temperature from room temperature to 60 °C with 20 ccm of gas flow rate. (a) Cell voltage and (b) power density.

Although the area power density of the miniaturized fuel cell was still low compared to aconventional fuel cell, the volumetric power density of 360 mW cm^{-3} was similar to a conventional fuel cell. The advantage of the silicon based miniaturized fuel cell is in its volumetric power density.

3.2.3. *Cell temperature control with a thin film heater*

The cell performance tests using a temperature control system were carried out with 20 ccm of hydrogen and oxygen at various temperatures. The slight increment of the open circuit voltage of the I–V curves in Fig. 8(a) was measured in accordance with increasing the cell temperature. This means that the oxidation/reduction reactions on both the catalyst layers were activated because of the cell heating from the thin-film heater. However, the ohmic loss increased dramatically according to the cell temperature from room temperature to 60 °C. The Nafion 112 membrane was not sufficiently hydrated due to a drying effect and, therefore, had a larger resistance to proton transfer. Thus, the operation of a single fuel cell without humidification at a higher temperature indicates a worse performance at 0.6 V; 171.0 mW cm^{-2} at room temperature, 129.5 mW cm^{-2} at 45 °C and 57.6 mW cm^{-2} at 60 °C. This tendency will be further studied with humidification tests.

4. Conclusions

A silicon-based miniature PEM fuel cell with a 4 cm^2 of active area was constructed and its electrochemical characteristics were investigated. The silicon separators played the roles of: gas distributor, current collector and heater for the anode and cathode and were fabricated by photolithography, KOH anisotropic wet etching, anodic bonding and DC sputtering. As a result, the single fuel cell with these separators appeared to have a practical power density of about 203 mW cm^{-2} at 0.6 V and a maximum power density of 261 mW cm^{-2} when it was operated at room temperature and ambient pressure with 20 ccm gas flow rates. The power density per cell volume was 360 mW cm^{-3}, which is similar to that of a conventional non-silicon fuel cell with pure gases and heating [13]. This indicates that a silicon separator can be successfully applied as an alternative to conventional bipolar plates for small PEM fuel cells because it has suitable properties, especially strength and conductivity from the anodic bonding and gold deposition processing. Furthermore, a significant cost reduction is also possible because it uses a continuous process with wet etching and can be applied to mass production.

Acknowledgments

This work was supported by the Research Center for Energy Conversion and Storage (RCECS), Seoul Renewable Energy Research Consortium (Seoul RERC) and the Inter-University Semiconductor Research Center (ISRC).

References

[1] L. Carrette, K.A. Friedrich, U. Stimming, Fuel Cells 1 (2001) 5–39.
[2] Larminie James, Dicks Andrew, Fuel Cell Systems Explained, John Wiley & Sons, Chichester, West Sussex, 2002.
[3] G.O. Mepsted, J.M. Moore, Handbook of Fuel Cells, vol. 3, John Wiley & Sons Ltd, Chichester, West Sussex, 2003, pp. 286–293.
[4] S.J. Lee, A. Chang-Chien, S.W. Cha, R. O'Hayer, Y.I. Park, Y. Saito, F.B. Prinz, J. Power Sources 112 (2002) 410–418.
[5] Yu Jingrong, Cheng Ping, Ma Zhiqi, Yi Baolian, J. Power Sources 124 (2003) 40–46.
[6] T. Pichonat, B. Gauthier-Menuel, D. Hauden, Chem. Eng. J. 101 (2004) 107–111.
[7] Kyong-Bok Min, Shuji Tanaka, Masayoshi Esashi, IEEE 6th Int. Conf. Micro Electro. Mech. Sys, 2003. pp. 379–382.
[8] Hayase Massanori, Kawase Takahiko, Hatsuzawa Takeshi, Electrochem. Solid State 7 (8) (2004) A231–A234.
[9] M. Elwenspoek, H.V. Jansen, Silicon Micromachining, Cambridge University Press, Trumpington Street, Cambridge, 1998.
[10] Oh Joong Kwon, Sun-Mi Hwang, Jin-Goo Ahn, Jae Jeong Kim, J. Power sources, in press.
[11] Huang Jianhua, Donald G. Baird, James E. McGrathb, J. Power Sources 150 (2005) 110–119.
[12] E.A. Cho, U.-S. Jeon, H.Y. Ha, S.-A. Hong, I.-H. Oh, J. Power Sources 125 (2004) 178–182.
[13] Chang-Soo Kim, Proceedings in New Trends in Fuel Cell Technology, Yonsei Engineering Research Complex, Seoul, 2005, pp. 111–125.